

# Electro-Functional Octupolar $\pi$ -Conjugated Columnar Liquid Crystals

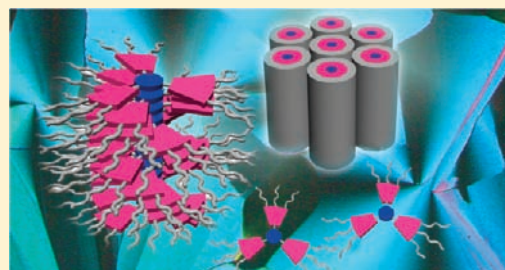
Takuma Yasuda,<sup>\*,†,§</sup> Tomohiro Shimizu,<sup>†</sup> Feng Liu,<sup>‡</sup> Goran Ungar,<sup>‡</sup> and Takashi Kato<sup>\*,†</sup>

<sup>†</sup>Department of Chemistry and Biotechnology, School of Engineering, The University of Tokyo, Hongo, Bunkyo-ku, Tokyo 113-8656, Japan

<sup>‡</sup>Department of Materials Science and Engineering, University of Sheffield, Mappin Street, Sheffield S1 3JD, United Kingdom

<sup>§</sup> Supporting Information

**ABSTRACT:** A series of propeller-shaped  $\pi$ -conjugated molecules based on 2,4,6-tris(thiophene-2-yl)-1,3,5-triazines has been designed and synthesized to obtain ambipolar charge-transferring liquid-crystalline materials. The 3-fold electron-donating aromatic units are attached to the electron-accepting triazine core, which forms electro-functional octupolar  $\pi$ -conjugated structures. These octupolar molecules self-organize into one-dimensional columnar nanostructures and exhibit ambipolar carrier transport behavior, which has been revealed by time-of-flight measurements. In this approach, electron-donor and acceptor electro-active segments are assembled individually in each column to give one-dimensional nanostructured materials with precisely tuned electronic properties. Their desirable electronic structures responsible for both hole and electron conduction have also been examined by cyclic voltammetry and theoretical calculations. The present results provide a new guideline and versatile approach to the design of ambipolar conductive nanostructured liquid-crystalline materials.



## INTRODUCTION

The controlled self-assembly of  $\pi$ -conjugated molecules into ordered supramolecular architectures is a subject of increasing research interest for the tailoring of their functionalities, and for application in organic electronic devices.<sup>1,2</sup> The induction of liquid crystallinity in  $\pi$ -conjugated materials is one of the promising approaches to control molecular self-organization processes, and thus to enhance the dynamic and anisotropic properties.<sup>3,4</sup> Among various functional soft materials, columnar liquid crystals<sup>3–9</sup> deserve particular attention because of their ability to form highly ordered one-dimensional (1D) superstructures that can be used for transportation of charges<sup>5</sup> and ions,<sup>6</sup> molecular separation,<sup>7</sup> catalysis,<sup>8</sup> and photonics applications.<sup>9</sup> Over the last two decades, discotic  $\pi$ -conjugated molecules such as triphenylenes,<sup>5a,b</sup> hexabenzocoronenes,<sup>5c–e</sup> and phthalocyanines<sup>5f</sup> have been well-established as columnar liquid-crystalline (LC) semiconductors. For the development of electro- and photofunctional columnar liquid crystals, it is crucial to design new  $\pi$ -conjugated structures and to fabricate nanostructured materials having accurate spatial arrangement of the functional entities. In this context, we previously reported that linear elongated  $\pi$ -conjugated oligothiophene derivatives self-assemble into columnar LC nanostructures and exhibit anisotropic functions.<sup>10</sup>

Recently, octupolar<sup>11</sup>  $\pi$ -conjugated molecules possessing electron donor–acceptor (D–A) hybrid characteristics have attracted much attention in a variety of research areas as promising materials for nonlinear optics (NLO).<sup>11,12</sup> However, to our knowledge, their potential usability for the application to charge-transporting materials has not been explored. Our design strategy here is to integrate the octupolar  $\pi$ -conjugated

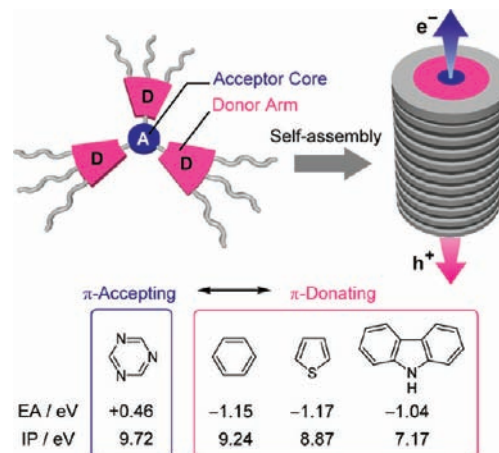


**Figure 1.** Design of the octupolar  $\pi$ -conjugated molecule and its self-assembled nanosegregated structure for ambipolar conductive columnar materials (top). Electronic properties of aromatic units (bottom). EA, electron affinity; IP, ionization potential.

molecules that consist of an acceptor core and peripheral multi-donor arms, into 1D columnar nanostructures for the development of electro-functional liquid crystals (Figure 1). The central 1,3,5-triazine core possesses an electron affinity considerably larger than those of other aromatic rings<sup>13</sup> and serves as an electron-accepting unit, whereas the thiophene-based

Received: April 17, 2011

Published: July 26, 2011

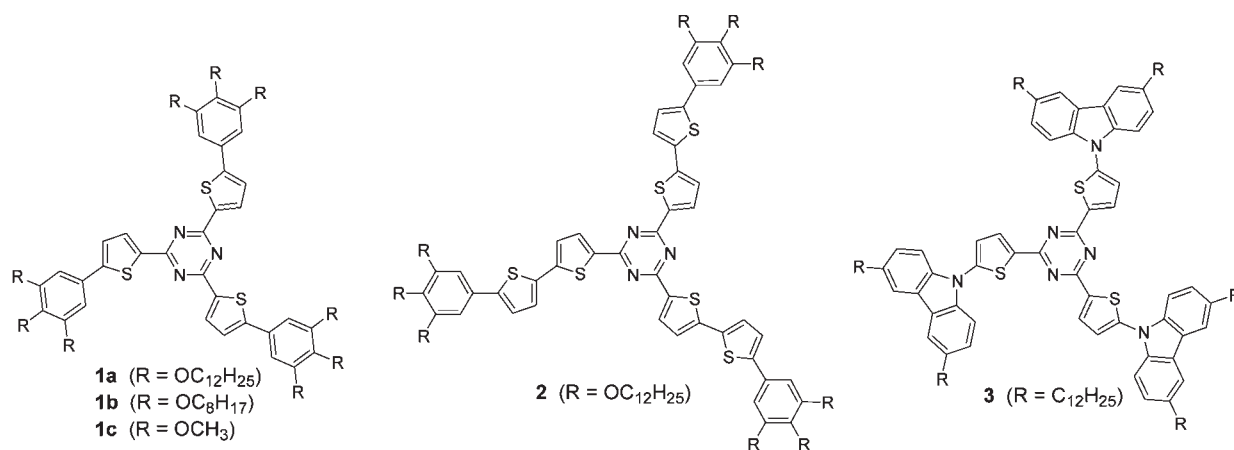


Figure 2. Chemical structures of 1,3,5-triazine-based octupolar  $\pi$ -conjugated molecules.

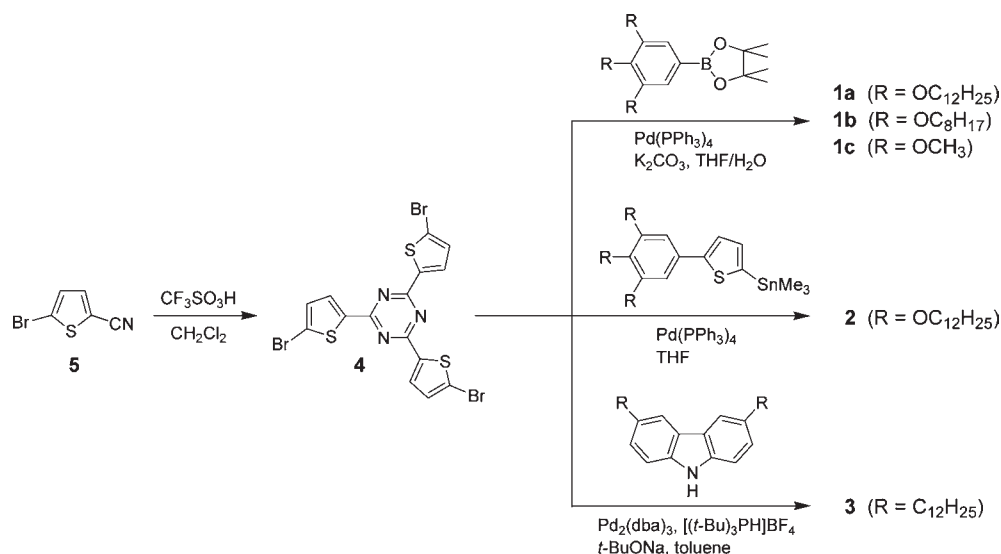


Figure 3. Synthetic routes for octupolar  $\pi$ -conjugated liquid crystals.

segments can provide electron-donating properties. These electronic and structural features can make these molecules promising as ambipolar charge-transporting LC materials. Some triazine-based columnar liquid crystals<sup>14</sup> and star-shaped columnar liquid crystals bearing different functional  $\pi$ -conjugated arms<sup>15</sup> have been developed; however, no ambipolar conduction behavior has been achieved in those columnar LC materials. Thus, it still remains a challenge to develop new processable ambipolar materials forming ordered LC states for optoelectronic applications.

We demonstrate here the first experimental study toward the realization of ambipolar conductive columnar materials by 1D self-organization of octupolar  $\pi$ -conjugated LC molecules **1–3** (Figure 2). In contrast to conventional linear-type D–A molecules, our new molecular design offers a possibility for the donor and acceptor electro-active constituents to stack individually in coaxial concentric shells to provide 1D hole and electron transport pathways in the columnar nanostructures. For these molecules, the electronic and photophysical properties can be tuned by merely changing the donor and/or acceptor motifs.

## RESULTS AND DISCUSSION

**Synthetic Strategy and Characterization.**  $\pi$ -Conjugated molecules **1–3** based on 1,3,5-triazine have been synthesized as shown in Figure 3. These compounds were obtained using the palladium-catalyzed 3-fold coupling methodology. The  $C_3$ -symmetrical precursor, 2,4,6-tris(5-bromothiophene-2-yl)-1,3,5-triazine (**4**), was prepared by trimerization of 5-bromothiophene-2-carbonitrile (**5**). Suzuki–Miyaura cross-coupling reactions<sup>16</sup> of tribromide **4** with 3 equiv of the corresponding phenylboronic esters afforded compounds **1a–c** in the presence of a catalytic amount of  $\text{Pd}(\text{PPh}_3)_4$ . Compound **2** possessing three phenylbithiophene arms was synthesized by the Stille cross-coupling reaction.<sup>17</sup> The carbazolyl-substituted compound **3** was obtained via Buchwald–Hartwig amination<sup>18</sup> using a mixture of  $\text{Pd}_2(\text{dba})_3$  (dba = *E,E*-dibenzylideneacetone) and  $[(t\text{-Bu})_3\text{PH}]\text{BF}_4$  as the catalyst.<sup>19</sup> In these experimental conditions, all of the final compounds were isolated in high yields (80–97%) after purification (see the Supporting Information for details). These compounds were readily soluble in common organic solvents by virtue of the attached flexible chains and were fully characterized by

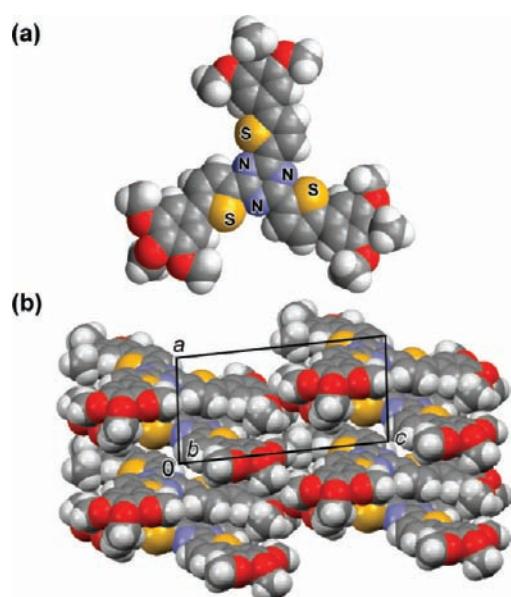


**Figure 4.** Space-filling representation of the crystal structure of **1c**: (a) molecular conformation with intramolecular  $S \cdots N$  interactions and (b) packing view along the  $b$ -axis. Atom color code: C, gray; N, blue; O, red; S, yellow. In the crystal packing, the molecules are rotationally displaced with respect to the adjacent molecules and are stacked via  $\pi$ - $\pi$  interactions along the  $a$ -axis.

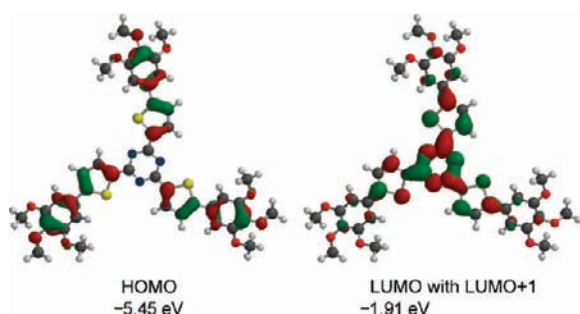


**Figure 5.** The frontier orbital distributions of **1c** calculated at the B3LYP/6-31G(d) level. The LUMO and LUMO+1 are degenerate.

$^1\text{H}$  and  $^{13}\text{C}$  NMR spectroscopy, matrix-assisted laser desorption ionization time-of-flight (MALDI-TOF) mass spectrometry, and elemental analysis.

**Crystal and Molecular Structures.** X-ray crystallographic analysis for compound **1c** with the terminal methoxy substituents provides useful insights into the self-assembled structures of the propeller-shaped  $\pi$ -conjugated molecules (Figure 4). The crystal structure of **1c** indicates that the molecule adopts a nearly planar conformation with dihedral angles between the central triazine and three thiophene rings in the range of  $1$ – $11^\circ$ . A fairly high degree of coplanarity in the whole molecule is attained through intramolecular nonbonded  $S \cdots N$  interactions,<sup>20</sup> in which the lone pair of  $sp^2$ -hybridized nitrogen atoms can interact with the unoccupied orbital on the neighboring sulfur atoms. The observed  $S \cdots N$  contact distances of  $2.9$ – $3.0$  Å are indeed shorter than the sum of the corresponding van der Waals radii ( $3.35$  Å).<sup>21</sup> Such attractive intramolecular interactions would restrict rotation of the nearby thiophene rings and allow an efficient 1D stacking of the propeller-shaped molecules (Figure 4b).

**Table 1.** Thermal Properties and XRD Data of Compounds **1**–**3**

compound	phase transition behavior <sup>a</sup>	XRD data	
		$T$ ( $^\circ\text{C}$ )	$a^b$ (Å)
<b>1a</b>	Cr 24 (6) Col <sub>h</sub> 107 (4) Iso	100	36.7
<b>1b</b>	Cr 25 (7) Col <sub>h</sub> 114 (2) Iso	100	31.9
<b>2</b>	Cr 48 (25) Col <sub>h</sub> 125 (31) Iso	110	45.0
<b>3</b>	G 8 Col 80 (3) Iso	70	34.4

<sup>a</sup> Transition temperatures ( $^\circ\text{C}$ ) and transition enthalpies ( $\text{kJ mol}^{-1}$ ) in parentheses, determined by DSC on heating. Cr, crystalline; G, glassy; Col<sub>h</sub>, hexagonal columnar; Col, columnar; Iso, isotropic. <sup>b</sup> Lattice parameters for the hexagonal ( $p6mm$ ) lattice.

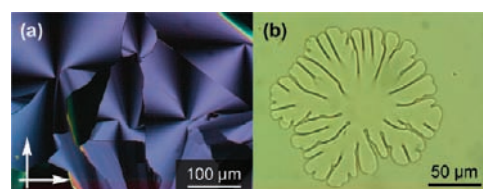


**Figure 6.** (a) Polarizing optical photomicrograph of **1b** in the Col<sub>h</sub> phase at  $100$   $^\circ\text{C}$ . (b) Dendritic growth of a homeotropic domain of **1b** on slow cooling ( $1$   $^\circ\text{C min}^{-1}$ ) with uncrossed polarizers. The arrows indicate the directions of polarizer and analyzer axes.

The intermolecular distance between the longitudinally stacked propellers is estimated to be  $3.5$ – $3.6$  Å, indicative of the existence of  $\pi$ - $\pi$  electronic interactions in the self-assembled structures.

The electro-active molecular structures have been examined by density-functional theory (DFT) calculations (Figure 5). In principle, carrier transport behavior is closely related to the electronic structures of the materials. The DFT studies on compound **1c**, which is the shorter chain homologue, reveal that the highest occupied molecular orbital (HOMO) is expanded over the peripheral three phenylthiophene arms, as seen in Figure 5. In contrast, the distributions of the lowest unoccupied molecular orbital (LUMO) and its degenerate orbital (LUMO+1) are mainly located on the central triazine core and fade out toward the periphery. Accordingly, the HOMO–LUMO photo-excited transitions in the octupolar molecules are accompanied by a displacement of the electron density from the three peripheral donor segments to the central acceptor core, resulting in an effective intramolecular charge transfer (ICT) through the  $\pi$ -conjugation framework.

**Liquid-Crystalline Properties.** The thermotropic liquid-crystalline (LC) properties of compounds **1**–**3** are summarized in Table 1. Compounds **1a,b** and **3** having flexible alkyl chains exhibit columnar LC phases from room temperature upon heating, while the columnar phase of **2** with an enlarged  $\pi$ -conjugated core exists over relatively higher temperatures in the range of  $48$ – $125$   $^\circ\text{C}$ . The isotropization temperature of **2** is about  $10$ – $20$   $^\circ\text{C}$  higher than those of **1a,b**. When the sample of **1b** is cooled from the isotropic state, a fan texture characteristic of a hexagonal columnar (Col<sub>h</sub>) phase is observed under polarizing optical microscope (Figure 6a). On slower cooling, dendritic growth of homeotropic Col<sub>h</sub> domains formed by **1b** is seen with uncrossed polarizers (Figure 6b) at the phase transition from the isotropic state. The transition enthalpy of **2** ( $\Delta H = 31$   $\text{kJ mol}^{-1}$ ) from the Col<sub>h</sub> to the



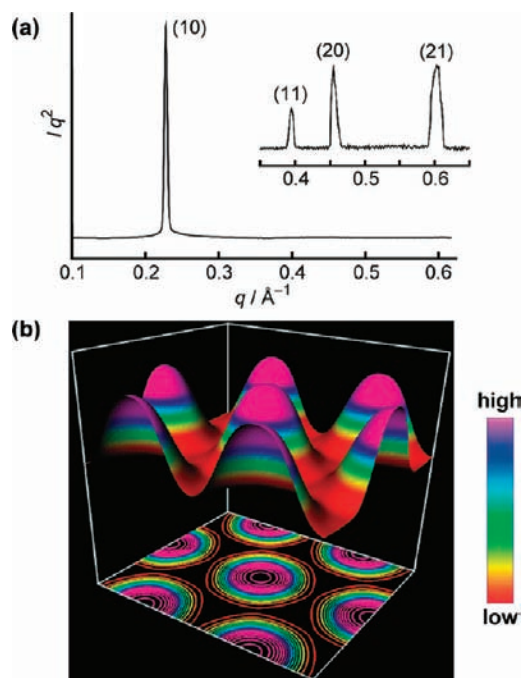


**Figure 7.** (a) High-resolution XRD pattern (small-angle region) of **1b** in the  $\text{Col}_h$  phase at 100 °C. The inset shows a magnified view. (b) Electron-density map (surface and contour plot) calculated from the XRD data.

isotropic phase is considerably larger than those observed for **1a,b** ( $\Delta H = 2\text{--}4 \text{ kJ mol}^{-1}$ ), implying the presence of well-organized molecular association in the  $\text{Col}_h$  phase of **2** as a consequence of enhanced intermolecular  $\pi\text{--}\pi$  interactions. The difference in the columnar packing mode of **2** is currently under study in detail.

To confirm the columnar LC structures, X-ray diffraction (XRD) measurements have been performed for **1–3** (Table 1, see also the Supporting Information). A representative XRD pattern for **1b** in the  $\text{Col}_h$  phase taken under synchrotron radiation is depicted in Figure 7a. In the small-angle region, one intense peak at 27.6 Å and three weak peaks at 16.0, 13.8, and 10.4 Å with the reciprocal  $d$ -spacing ratio of  $1:3^{1/2}:2:7^{1/2}$  are observed. These peaks are indexed as (10), (11), (20), and (21) reflections of a two-dimensional hexagonal ( $p6mm$ ) lattice. In the wide-angle region, two diffuse peaks are also observed at 4.0 and 3.3 Å (see the Supporting Information for details). These peaks should come from the peripheral alkyl chains and  $\pi\text{--}\pi$  stacking of the adjacent aromatic cores.

The formation of the  $\text{Col}_h$  structures is further supported by the electron-density map (Figure 7b) that has been reconstructed from the XRD data. In the density map, each supramolecular column indeed has a circular cross section with high electron density (purple/blue) that should be dominated by the electron-rich  $\pi$ -conjugated cores. The terminal aliphatic chains are located in the low electron-density moats (yellow/red) surrounding the  $\pi$ -conjugated cores. Accordingly, the propeller-shaped molecules would stack successively with a rotation along the column axis to fill the allotted space inside the column (Figure 8). The nanosegregation of the  $\pi$ -conjugated cores from the surrounding flexible chains as well as longitudinal intermolecular  $\pi\text{--}\pi$  interactions cooperatively facilitate the organization of the molecules into the columnar nanostructures. The  $\text{Col}_h$  structures of the homologous compounds are similar to that described for **1b**, while the intercolumnar distance increases from 31.9 Å (for **1b**) through 36.7 Å (for **1a**) to 45.0 Å

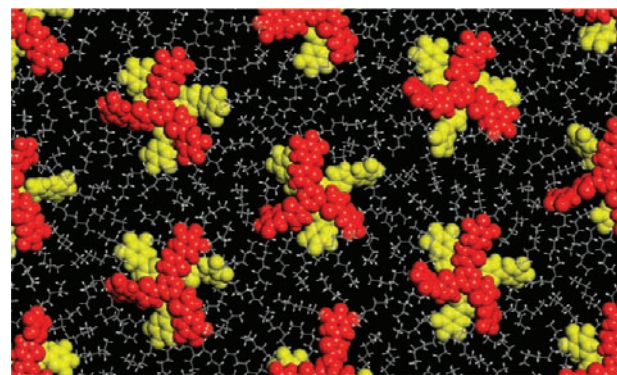


**Figure 8.** Representation of a hexagonal columnar nanostructure of **1b** (density =  $0.98 \text{ g cm}^{-3}$ ) using molecular dynamics simulation. The  $\pi$ -conjugated aromatic cores and alkyl chains are shown with space-filling and stick models, respectively.

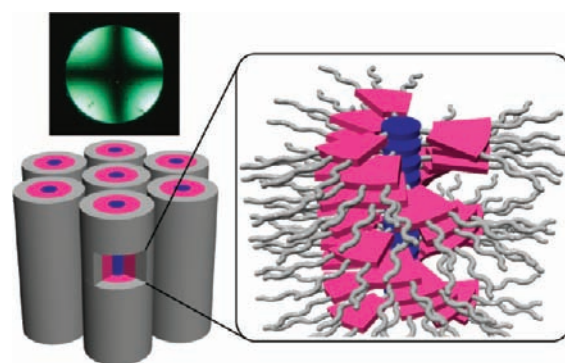


**Figure 9.** Schematic illustration of the homeotropically aligned  $\text{Col}_h$  structure of **1a**. The blue, pink, and gray portions stand for the triazine cores, phenylthiophene units, and alkyl chains, respectively. The conoscopic image of **1a** at 100 °C in an ITO cell is also shown.

(for **2**) upon elongation of the alkyl chain and/or the  $\pi$ -conjugated core (Table 1). The intercolumnar distance of **1b** estimated from the XRD data is shorter than the calculated molecular length (ca. 37 Å) because of the interdigitation of the outer chains between the neighboring columns.

**Charge Carrier Transport Properties.** The well-organized columnar nanostructures, which are composed of extended  $\pi$ -stacks of the molecules, can provide 1D pathways for mobile charge carriers. To evaluate the carrier transport properties of **1–3**, time-of-flight (TOF) measurements have been performed for the compounds in the LC states (see the Supporting Information for details). We have prepared cells filled with the LC samples between two indium–tin–oxide (ITO)-coated glass electrodes. Compounds **1a,b** and **2** spontaneously align in a homeotropic manner such that the columns run between the electrodes in the cell without surface treatment. The homeotropic alignment has been confirmed by the observation of a cross-shaped conoscopic interference pattern with a polarizing microscope (Figure 9). This propensity of the propeller-shaped molecules to self-organize into a large columnar domain with a face-on alignment increases the applicability to 1D conductive materials. In contrast, compound **3** does not show such a tendency toward spontaneous homeotropic alignment in the  $\text{Col}$  phase.

Figure 10 displays the transient photocurrent curves for holes and electrons, respectively, in the  $\text{Col}_h$  phase of **1a** under different

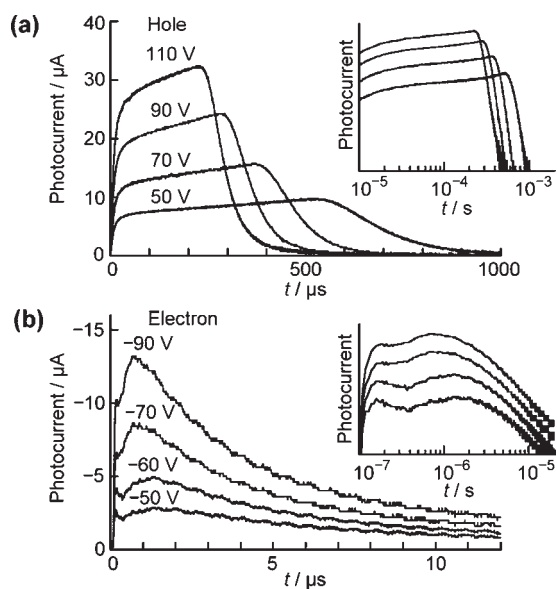


**Figure 10.** Transient photocurrent curves for (a) holes and (b) electrons in the Col<sub>h</sub> phase of **1a** at 100 °C. The insets display double-logarithmic plots.

applied voltages. The photocurrents for holes exhibit a characteristic plateau and a well-defined transit, whereas those for electrons are relatively dispersive presumably due to trap sites formed by oxygen.<sup>22</sup> The transit time for the photogenerated charge carriers consistently increases upon reducing the applied electric-field strength. These observations unambiguously indicate the occurrence of both hole and electron conduction, that is, ambipolar carrier transport, in the octupolar  $\pi$ -conjugated LC materials. It is noteworthy that such an ambipolar conductive behavior is uncommon in the general case of single component organic materials. Only a few examples of LC semiconductors such as triphenylenes<sup>23a–c</sup> and oligothiophenes<sup>23d–g</sup> exhibiting ambipolar characteristics have been reported. On the basis of the TOF data (Figure 10), the hole and electron mobilities of **1a** are calculated to be  $\mu_+ = 3 \times 10^{-5}$  and  $\mu_- = 4 \times 10^{-3} \text{ cm}^2 \text{ V}^{-1} \text{ s}^{-1}$  at 100 °C, respectively. Compound **1b** also exhibits ambipolar conduction behavior, giving rise to hole and electron mobilities on the order of  $10^{-5}$  and  $10^{-3} \text{ cm}^2 \text{ V}^{-1} \text{ s}^{-1}$ , respectively, in the Col<sub>h</sub> phase (Supporting Information). These mobilities are nearly field-independent in the accessible electric-field ranges ( $5 \times 10^4$  to  $1 \times 10^5 \text{ V cm}^{-1}$ ).

The photoconductive properties of **1–3** have been further examined over a range of temperatures. The results for their carrier mobilities as a function of temperature are shown in Figure 11. In the isotropic phase of **1a**, quite low carrier mobilities on the order of  $10^{-6} \text{ cm}^2 \text{ V}^{-1} \text{ s}^{-1}$  are observed, which can be rationalized with Arrhenius-type temperature dependence. As for compound **1a**, the hole and electron mobilities (○ and ● in Figure 11) discontinuously increase by about 1 and 3 orders of magnitude, respectively, at the isotropic–Col<sub>h</sub> phase transition upon cooling, reflecting the formation of ordered 1D  $\pi$ -stacked structures in the Col<sub>h</sub> phase.

Remarkably, the transport of electrons in the Col<sub>h</sub> phases of **1a,b** is more than 100-times faster than that of holes. We infer that this behavior should originate from the octupolar structure of the propeller-shaped molecules containing both the electron-accepting triazine core and the trigonally ramified electron-donating phenylthiophene units (vide infra). In the Col<sub>h</sub> phases, the triazine cores stack one another in the center of the columns (the blue parts

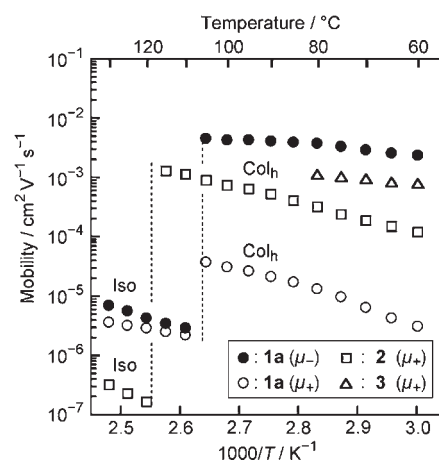


**Figure 11.** Temperature dependence of carrier mobilities of **1a**, **2**, and **3** upon cooling: (●) electrons and (○) holes for **1a** at  $1.0 \times 10^5 \text{ V cm}^{-1}$ ; (□) holes for **2** at  $1.0 \times 10^5 \text{ V cm}^{-1}$ ; (△) holes for **3** at  $1.3 \times 10^5 \text{ V cm}^{-1}$ . The dashed lines denote the isotropic–Col<sub>h</sub> phase transition upon cooling.

in Figure 9), thereby providing efficient 1D electron-transporting n-channels with relatively high electron mobilities. The observed electron mobilities of **1a,b** ( $\mu_- = 10^{-2}–10^{-3} \text{ cm}^2 \text{ V}^{-1} \text{ s}^{-1}$ ) in the nanostructured LC states are 1–4 orders of magnitude higher than those of widely used electron-transporting amorphous materials,<sup>24</sup> including tris(8-hydroxyquinoline)aluminum (Alq<sub>3</sub>),<sup>22,25a–25c</sup> 1,3,4-oxadiazole derivatives,<sup>25d</sup> and other 1,3,5-triazine derivatives.<sup>26</sup> On the other hand, the relatively low hole mobilities observed for **1a,b** are ascribed to less effective  $\pi$ -overlap of the electron-donating phenylthiophene segments (the pink parts in Figure 9) between the nearby molecules because the propeller-shaped molecules can rotate around the column axis even in the Col<sub>h</sub> phases.<sup>27</sup> Thus, it is conceivable that hopping of holes should become slower under the influence of the energy barriers (energetic disorder) produced by the rotational displacement of the  $\pi$ -conjugated units along the column.

For compounds **2** and **3**, no distinct electron mobility could be evaluated due to highly dispersive features of the photocurrents in the experimental conditions. However, the hole mobilities of both **2** and **3** (□ and △ in Figure 11) in the Col phases are found to be higher than those of **1a,b** and reach values of  $\mu_+ = 1 \times 10^{-3} \text{ cm}^2 \text{ V}^{-1} \text{ s}^{-1}$ . The enhanced hole mobilities in **2** and **3** as compared to **1a,b** may arise from an increased intermolecular  $\pi$ -overlap attributed to the expanded electron-donating segments (the phenylbithiophene units in **2** and the carbazolythiophene units in **3**) within the columns.

**Photophysical and Electrochemical Properties.** To clarify the photophysical properties, UV/vis absorption and photoluminescence (PL) spectra of **1–3** have been measured both in solutions and in LC films on quartz substrates (Figure 12 and the Supporting Information). The photophysical data are also summarized in Table 2. The lowest energy absorption maxima ( $\lambda_{\text{abs}}$ ) of **1a**, **2**, and **3** are observed at 385, 440, and 415 nm, respectively, in the Col phases. The red-shifted absorption of **2** ( $\lambda_{\text{abs}} = 440 \text{ nm}$ ) in comparison with **1a** ( $\lambda_{\text{abs}} = 385 \text{ nm}$ ) should be attributed to its extended  $\pi$ -conjugation length. Moreover, in the condensed LC state, the absorption spectrum of **2** becomes broader as compared to that observed in solution, indicating the occurrence of intermolecular electronic interactions. As for **3**, the replacement of the outermost phenyl groups of **1a** by *N*-carbazolyl units results in

Table 2. Photophysical and Electrochemical Data of Compounds 1–3

	UV/vis $\lambda_{\max}$ (nm)		photoluminescence $\lambda_{\text{em}}$ (nm)			redox potential <sup>c</sup> (V)				
	CH <sub>2</sub> Cl <sub>2</sub> <sup>a</sup>	LC film <sup>b</sup>	CH <sub>2</sub> Cl <sub>2</sub> <sup>a</sup>	LC film <sup>b</sup>	Stokes shift <sup>a</sup> (nm)	$E_{\text{ox}}$	$E_{\text{red}}$	$E_{\text{HOMO}}^d$ (eV)	$E_{\text{LUMO}}^e$ (eV)	$E_g^f$ (eV)
<b>1a</b>	392	385	528	519	6600	+0.79	−2.20	−5.46	−2.90	2.56
<b>1b</b>	392	385	528	521	6600	+0.80	−2.19	−5.46	−2.90	2.56
<b>2</b>	434	440	560	585	5200	+0.61	−2.04	−5.24	−3.03	2.21
<b>3</b>	296, 415	299, 415	503	490	4200	+0.78	−2.13	−5.37	−3.00	2.37

<sup>a</sup> Measured in CH<sub>2</sub>Cl<sub>2</sub> solution ( $1 \times 10^{-5}$  M) at room temperature. <sup>b</sup> Measured in the Col phases at 90 °C for **1a,b**, at 110 °C for **2**, and at 70 °C for **3**. <sup>c</sup> Determined by cyclic voltammetry in CH<sub>2</sub>Cl<sub>2</sub> solution of Bu<sub>4</sub>NClO<sub>4</sub> (0.10 M).  $E_{\text{ox}}$  and  $E_{\text{red}}$  stand for oxidation peak and reduction peak potentials, respectively, vs Fc<sup>+</sup>/Fc. <sup>d</sup> Calculated from the onset oxidation potential with the assumption that the energy level of ferrocene is 4.8 eV below vacuum level:  $E_{\text{HOMO}} = -E_{\text{onset(ox)}} - 4.8$  eV. <sup>e</sup> Calculated from the onset reduction potential:  $E_{\text{LUMO}} = -E_{\text{onset(red)}} - 4.8$  eV. <sup>f</sup> HOMO–LUMO energy gap according to  $E_g = E_{\text{LUMO}} - E_{\text{HOMO}}$ .

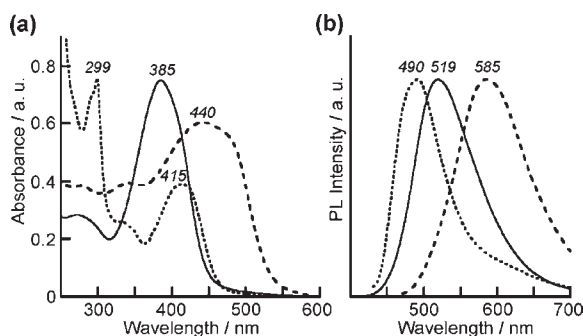


Figure 12. (a) UV/vis absorption and (b) photoluminescence spectra of **1a** (—), **2** (---), and **3** (· · ·) in the Col phases.

a bathochromic shift of  $\lambda_{\text{abs}}$  by 30 nm despite the disruption of  $\pi$ -conjugation in the molecule.

It has been revealed that the PL emission color of the octupolar LC materials can be tuned from blue-green to orange by changing the electron-donating segments (Figure 12b). Compound **3** in the Col phase exhibits an emission maximum ( $\lambda_{\text{em}}$ ) at 490 nm, which takes place at a higher energy with a smaller Stokes shift than those of **1a** ( $\lambda_{\text{em}} = 519$  nm) and **2** ( $\lambda_{\text{em}} = 585$  nm). This result suggests that the electron-donating *N*-carbazolyl units in **3** can behave as a fairly independent electronic entity<sup>28</sup> and should not possess strong electronic coupling toward the triazine-based core.

The redox properties of **1–3** have been characterized by cyclic voltammetry, as listed in Table 2 (see also the Supporting Information). It has been demonstrated that all of the compounds undergo both electrochemical oxidation and reduction processes because of their D–A hybrid characteristics. Compound **2** having the phenylbithiophene arms is more easily oxidized and presents an oxidation peak ( $E_{\text{ox}}$ ) at 0.61 V vs ferrocenium/ferrocene (Fc<sup>+</sup>/Fc), which is about 0.2 V less positive than **1a,b** and **3**. Upon scanning in the negative potential region for **1–3**, a reduction peak ( $E_{\text{red}}$ ) assigned to the reduction of the triazine core appears in the range from −2.0 to −2.2 V vs Fc<sup>+</sup>/Fc. The HOMO and LUMO energy levels ( $E_{\text{HOMO}}$  and  $E_{\text{LUMO}}$ ) can be estimated from the onset potentials of oxidation and reduction waves, respectively (Table 2), with the premise that the energy level of Fc is 4.8 eV below the vacuum level.<sup>29</sup> All of the compounds possess low-lying  $E_{\text{LUMO}}$  values of approximately −3.0 eV, which are comparable to that of Alq<sub>3</sub>,<sup>25c</sup> one of the most widely used electron-transporting materials.

## CONCLUSIONS

We have designed and synthesized a new class of nanostructured columnar liquid crystals based on octupolar  $\pi$ -conjugated structures, where three electron-donating segments are symmetrically attached to an electron-accepting triazine core. We have elucidated the influence of the molecular design on photoconductive properties and self-organizing behavior of the octupolar columnar liquid crystals. The time-of-flight experiments have revealed that these molecules are capable of transporting both holes and electrons in the columnar phases, functioning as ambipolar 1D conductive materials. The strong electron-accepting capability of the triazine core results in an intramolecular charge-transfer, leading to such ambipolar charge transport properties. The structural versatility of our molecular design can contribute to the further development of electro-functional LC materials with tailor-made properties. We envisage that octupolar  $\pi$ -conjugated liquid crystals will be new promising functional soft materials for applications in optoelectronic devices, such as organic light-emitting diodes, ambipolar field-effect transistors, and photovoltaic cells.

## ASSOCIATED CONTENT

**S Supporting Information.** Experimental details, <sup>1</sup>H NMR spectra, polarizing photomicrographs, DSC thermograms, WAXD patterns, TOF data, UV/vis and PL spectra, cyclic voltammograms of **1–3**, and crystallographic information file (CIF) of **1c**. This material is available free of charge via the Internet at <http://pubs.acs.org>.

## AUTHOR INFORMATION

### Corresponding Author

yasuda@cstf.kyushu-u.ac.jp; kato@chiral.t.u-tokyo.ac.jp

### Present Addresses

<sup>S</sup>Department of Applied Chemistry, Kyushu University, Motoooka, Nishi-ku, Fukuoka 819-0395, Japan.

## ACKNOWLEDGMENT

This study was partially supported by a Grant-in-Aid for the Global COE Program for Chemistry Innovation through Cooperation of Science and Engineering (T.K.), Grant-in-Aid for Innovation Areas “Fusion Materials” (No. 2206; T.K.), and Exploratory Research (No. 22655061; T.K.) from the Ministry



of Education, Culture, Sports, Science and Technology, Japan. G.U. acknowledges support from the WCU program through the National Research Foundation of Korea funded by the Ministry of Education, Science and Technology (R31-10013), and the European FP7 project NANOGOLD. We would like to thank Dr. Masahiro Funahashi, Dr. Tatsuya Nishimura, and Dr. Xiangbing Zeng for helpful discussions, Dr. Makoto Yamashita for support in crystallographic analysis, and Ms. Kimiyo Saeki for elemental analysis at the University of Tokyo. T.Y. is grateful for financial support from the JSPS Research Fellowship for Young Scientists and the Mitsubishi Chemical Corp. Fund. We thank Dr. Nick Terrill and Dr. Jen Hiller for their help with the synchrotron experiments at Diamond.

## REFERENCES

- (1) (a) Special Issue on "Supramolecular Chemistry and Self-Assembly". *Science* **2002**, *295*, 2395–2421. (b) Special Issue on "Supramolecular Approaches to Organic Electronics and Nanotechnology". *Adv. Mater.* **2006**, *18*, 1227–1329.
- (2) For reviews, see: (a) Pisula, W.; Feng, X.; Müllen, K. *Adv. Mater.* **2010**, *22*, 3634–3649. (b) Hoeben, F. J. M.; Jonkheijm, P.; Meijer, E. W.; Schenning, A. P. H. J. *Chem. Rev.* **2005**, *105*, 1491–1546. (c) Wu, J.; Pisula, W.; Müllen, K. *Chem. Rev.* **2007**, *107*, 718–747. (d) Kato, T.; Mizoshita, N.; Kishimoto, K. *Angew. Chem., Int. Ed.* **2006**, *45*, 38–68. (e) Elemans, J. A. A. W.; van Hameren, R.; Nolte, R. J. M.; Rowan, A. E. *Adv. Mater.* **2006**, *18*, 1251–1266. (f) Palmer, L. C.; Stupp, S. I. *Acc. Chem. Res.* **2008**, *41*, 1674–1684. (g) Nguyen, T.-Q.; Martel, R.; Bushey, M.; Avouris, P.; Carlsen, A.; Nuckolls, C.; Brus, L. *Phys. Chem. Chem. Phys.* **2007**, *9*, 1515–1532. (h) Würthner, F. *Chem. Commun.* **2004**, 1564–1579. (i) Thomas, S. W., III; Joly, G. D.; Swager, T. M. *Chem. Rev.* **2007**, *107*, 1339–1386. (j) Ajayaghosh, A.; Praveen, V. K. *Acc. Chem. Res.* **2007**, *40*, 644–656. (k) Gin, D. L.; Pecinovsky, C. S.; Bara, J. E.; Kerr, R. L. *Struct. Bonding (Berlin)* **2008**, *128*, 181–222. (l) Kato, T. *Angew. Chem., Int. Ed.* **2010**, *49*, 7847–7848.
- (3) Demus, D.; Goodby, J. W.; Gray, G. W.; Spiess, H.-W.; Vill, V. *Handbook of Liquid Crystals*; Wiley-VCH: Weinheim, Germany, 1998.
- (4) For recent reviews on liquid crystals, see: (a) Goodby, J. W.; Saez, I. M.; Cowling, S. J.; Görtz, V.; Draper, M.; Hall, A. W.; Sia, S.; Cosquer, G.; Lee, S.-E.; Raynes, E. P. *Angew. Chem., Int. Ed.* **2008**, *47*, 2754–2787. (b) Laschat, S.; Baro, A.; Steinke, N.; Giesselmann, F.; Hägele, C.; Scalia, G.; Judele, R.; Kapatsina, E.; Sauer, S.; Schreivogel, A.; Tosoni, M. *Angew. Chem., Int. Ed.* **2007**, *46*, 4832–4887. (c) Sergeev, S.; Pisula, W.; Geerts, Y. H. *Chem. Soc. Rev.* **2007**, *36*, 1902–1929. (d) Tschierske, C. *Chem. Soc. Rev.* **2007**, *36*, 1930–1970. (e) Donnio, B.; Buathong, S.; Bury, I.; Guillon, D. *Chem. Soc. Rev.* **2007**, *36*, 1495–1513. (f) Pisula, W.; Zorn, M.; Chang, J. Y.; Müllen, K.; Zentel, R. *Macromol. Rapid Commun.* **2009**, *30*, 1179–1202. (g) Shimizu, Y.; Oikawa, K.; Nakayama, K.; Guillon, D. *J. Mater. Chem.* **2007**, *17*, 4223–4229. (h) Deschenaux, R.; Donnio, B.; Guillon, D. *New J. Chem.* **2007**, *31*, 1064–1073. (i) Kato, T.; Tanabe, K. *Chem. Lett.* **2009**, *38*, 634–639. (j) Lehmann, M. *Chem.-Eur. J.* **2009**, *15*, 3638–3651. (k) Kato, T.; Yasuda, T.; Kamikawa, Y.; Yoshio, M. *Chem. Commun.* **2009**, 729–739. (l) Kato, T.; Fréchet, J. M. J. *Liq. Cryst.* **2006**, *33*, 1429–1437.
- (5) (a) Boden, N.; Bushby, R. J.; Clements, J. J. *Chem. Phys.* **1993**, *98*, 5920–5931. (b) Adam, D.; Schuhmacher, P.; Simmerer, J.; Häussling, L.; Siemensmeyer, K.; Etbachi, K. H.; Ringsdorf, H.; Haarer, D. *Nature* **1994**, *371*, 141–143. (c) van de Craats, A. M.; Warman, J. M.; Müllen, K.; Geerts, Y.; Brand, J. D. *Adv. Mater.* **1998**, *10*, 36–38. (d) Shklyarevskiy, I. O.; Jonkheijm, P.; Stutzmann, N.; Wasserberg, D.; Wondergem, H. J.; Christianen, P. C. M.; Schenning, A. P. H. J.; de Leeuw, D. M.; Tomović, Ž.; Wu, J.; Müllen, K.; Maan, J. C. J. *Am. Chem. Soc.* **2005**, *127*, 16233–16237. (e) Xiao, S.; Myers, M.; Miao, Q.; Sanaur, S.; Pang, K.; Steigerwald, M. L.; Nuckolls, C. *Angew. Chem., Int. Ed.* **2005**, *44*, 7390–7394. (f) Ban, K.; Nishizawa, K.; Ohta, K.; van de Craats, A. M.; Warman, J. M.; Yamamoto, I.; Shirai, H. *J. Mater. Chem.* **2001**, *11*, 321–331. (g) Isoda, K.; Yasuda, T.; Kato, T. *Chem. Asian J.* **2009**, *4*, 1619–1625. (h) Percec, V.; Glodde, M.; Bera, T. K.; Miura, Y.; Shiyonovskaya, L.; Singer, K. D.; Balagurusamy, V. S. K.; Heiney, P. A.; Schnell, I.; Rapp, A.; Spiess, H.-W.; Hudson, S. D.; Duan, H. *Nature* **2002**, *419*, 384–387.
- (6) (a) Yoshio, M.; Mukai, T.; Ohno, H.; Kato, T. *J. Am. Chem. Soc.* **2004**, *126*, 994–995. (b) Shimura, H.; Yoshio, M.; Hoshino, K.; Mukai, T.; Ohno, H.; Kato, T. *J. Am. Chem. Soc.* **2008**, *130*, 1759–1765. (c) Cho, B.-K.; Jain, A.; Gruner, S. M.; Wiesner, U. *Science* **2004**, *305*, 1598–1601.
- (7) (a) Gin, D. L.; Lu, X.; Nemade, P. R.; Pecinovsky, C. S.; Xu, Y.; Zhou, M. *Adv. Funct. Mater.* **2006**, *16*, 865–878. (b) Gin, D. L.; Bara, J. E.; Noble, R. D.; Elliott, B. J. *Macromol. Rapid Commun.* **2008**, *29*, 367–389.
- (8) Xu, Y.; Gu, W.; Gin, D. L. *J. Am. Chem. Soc.* **2004**, *126*, 1616–1617.
- (9) (a) Hassheider, T.; Benning, S. A.; Kitzlerow, H.-S.; Achard, M.-F.; Bock, H. *Angew. Chem., Int. Ed.* **2001**, *40*, 2060–2063. (b) Schmidt-Mende, L.; Fechtenkötter, A.; Müllen, K.; Moons, E.; Friend, R. H.; MacKenzie, J. D. *Science* **2001**, *293*, 1119–1122. (c) O'Neill, M.; Kelly, S. M. *Adv. Mater.* **2003**, *15*, 1135–1146. (d) Sagara, Y.; Kato, T. *Angew. Chem., Int. Ed.* **2008**, *47*, 5175–5178. (e) Sagara, Y.; Kato, T. *Nat. Chem.* **2009**, *1*, 605–610. (f) Diring, S.; Camerel, F.; Donnio, B.; Dintzer, T.; Toffanin, S.; Capelli, R.; Muccini, M.; Ziesel, R. *J. Am. Chem. Soc.* **2009**, *131*, 18177–18185.
- (10) (a) Yasuda, T.; Ooi, H.; Morita, J.; Akama, Y.; Minoura, K.; Funahashi, M.; Shimomura, T.; Kato, T. *Adv. Funct. Mater.* **2009**, *19*, 411–419. (b) Minoura, K.; Akama, Y.; Morita, J.; Yasuda, T.; Kato, T.; Shimomura, T. *J. Appl. Phys.* **2009**, *105*, 113513–1–6. (c) Yasuda, T.; Kishimoto, K.; Kato, T. *Chem. Commun.* **2006**, 3399–3401.
- (11) (a) Zyss, J.; Ledoux, I. *Chem. Rev.* **1994**, *94*, 77–105. (b) Kim, H. M.; Cho, B. R. *J. Mater. Chem.* **2009**, *19*, 7402–7409.
- (12) (a) Chérioux, F.; Maillotte, H.; Audebert, P.; Zyss, J. *Chem. Commun.* **1999**, 2083–2084. (b) Cho, B. R.; Son, K. H.; Lee, S. H.; Song, Y.-S.; Lee, Y.-K.; Jeon, S.-J.; Choi, J. H.; Lee, H.; Cho, M. *J. Am. Chem. Soc.* **2001**, *123*, 10039–10045. (c) Hennrich, G.; Asselberghs, I.; Clays, K.; Persoons, A. *J. Org. Chem.* **2004**, *69*, 5077–5081. (d) Rupert, B. L.; Mitchell, W. J.; Ferguson, A. J.; Köse, M. E.; Rance, W. L.; Rumbles, G.; Ginley, D. S.; Shaheen, S. E.; Kopidakis, N. *J. Mater. Chem.* **2009**, *19*, 5311–5324. (e) Zou, L.; Liu, Z.; Yan, X.; Liu, Y.; Fu, Y.; Liu, J.; Huang, Z.; Chen, X.; Qin, J. *Eur. J. Org. Chem.* **2009**, 5587–5593. (f) Roquet, S.; Cravino, A.; Leriche, P.; Alévèque, O.; Frère, P.; Roncali, J. *J. Am. Chem. Soc.* **2006**, *128*, 3459–3466. (g) Inomata, H.; Goushi, K.; Masuko, T.; Konno, T.; Imai, T.; Sasabe, H.; Brown, J. J.; Adachi, C. *Chem. Mater.* **2004**, *16*, 1285–1291.
- (13) (a) Nenner, I.; Schultz, G. J. *J. Chem. Phys.* **1975**, *62*, 1747–1758. (b) Jordan, K. D.; Burrow, P. D. *Acc. Chem. Res.* **1978**, *11*, 341–348. (c) Barrio, L.; Catalán, J.; de Paz, J. L. G. *Int. J. Quantum Chem.* **2003**, *91*, 432–437. (d) Schwab, P. F. H.; Smith, J. R.; Michl, J. *Chem. Rev.* **2005**, *105*, 1197–1280.
- (14) (a) Goldmann, D.; Dietel, R.; Janietz, D.; Schmidt, C.; Wendorff, J. H. *Liq. Cryst.* **1998**, *24*, 407–411. (b) Lee, C.-H.; Yamamoto, T. *Tetrahedron Lett.* **2001**, *42*, 3993–3996. (c) Shu, W.; Valiyaveetil, S. *Chem. Commun.* **2002**, 1350–1351. (d) Bock, H.; Babeau, A.; Seguy, I.; Jolinat, P.; Destruel, P. *ChemPhysChem* **2002**, *532*–535. (e) Pieterse, K.; Lauritsen, A.; Schenning, A. P. H. J.; Vekemans, J. A. J. M.; Meijer, E. W. *Chem.-Eur. J.* **2003**, *9*, 5597–5604. (f) Zhang, Y.-D.; Jespersen, K. G.; Kempe, M.; Kornfield, J. A.; Barlow, S.; Kippelen, B.; Marder, S. R. *Langmuir* **2003**, *19*, 6534–6536. (g) Barberá, J.; Puig, L.; Serrano, J. L.; Sierra, T. *Chem. Mater.* **2004**, *16*, 3308–3317. (h) Lee, H.; Kim, D.; Lee, H.-K.; Qiu, W.; Oh, N.-K.; Zin, W.-C.; Kim, K. *Tetrahedron Lett.* **2004**, *45*, 1019–1022. (i) Holst, H. C.; Pakula, T.; Meier, H. *Tetrahedron* **2004**, *60*, 6765–6775. (j) Meier, H.; Lehmann, M.; Holst, H. C.; Schwöppe, D. *Tetrahedron* **2004**, *60*, 6881–6888.
- (15) (a) Pesak, D. J.; Moore, J. S. *Angew. Chem., Int. Ed. Engl.* **1997**, *36*, 1636–1639. (b) Meier, H.; Lehmann, M.; Kolb, U. *Chem.-Eur. J.* **2000**, *6*, 2462–2469. (c) Kim, B. G.; Kim, S.; Park, S. Y. *Tetrahedron Lett.* **2001**, *42*, 2697–2699. (d) Geng, Y.; Fechtenkötter, A.; Müllen, K. *J. Mater. Chem.* **2001**, *11*, 1634–1641. (e) Attias, A.-J.; Cavalli, C.; Donnio, B.; Guillon, D.; Hapiot, P.; Malthête, J. *Chem. Mater.* **2002**, *14*, 375–384. (f) Kimura, M.; Narikawa, H.; Ohta, K.; Hanabusa, K.; Shirai, H.; Kobayashi, N. *Chem. Mater.* **2002**, *14*, 2711–2717.

(g) Lehmann, M.; Köhn, C.; Meier, H.; Renker, S.; Oehlhof, A. *J. Mater. Chem.* **2006**, *16*, 441–451. (h) Hennrich, G.; Cavero, E.; Barberá, J.; Gómez-Lor, B.; Hanes, R. E.; Talarico, M.; Golemme, A.; Serrano, J. L. *Chem. Mater.* **2007**, *19*, 6068–6070. (i) Varghese, S.; Kumar, N. S. S.; Krishna, A.; Rao, D. S. S.; Prasad, S. K.; Das, S. *Adv. Funct. Mater.* **2009**, *19*, 2064–2073. (j) Kimura, M.; Hatano, T.; Yasuda, T.; Morita, J.; Akama, Y.; Minoura, K.; Shimomura, T.; Kato, T. *Chem. Lett.* **2009**, *38*, 800–801. (k) Tanabe, K.; Yasuda, T.; Kato, T. *Chem. Lett.* **2008**, *37*, 1208–1209. (l) Tomović, Ž.; van Dongen, J.; George, S. J.; Xu, H.; Pisula, W.; Leclère, P.; Smulders, M. M. J.; De Feyter, S.; Meijer, E. W.; Schenning, A. P. H. J. *J. Am. Chem. Soc.* **2007**, *129*, 16190–16196. (m) Luo, J.; Zhao, B.; Chan, H. S. O.; Chi, C. *J. Mater. Chem.* **2010**, *20*, 1932–1941. (n) Kanibolotsky, A. L.; Perepichka, I. F.; Skabara, P. J. *Chem. Soc. Rev.* **2010**, *39*, 2695–2728. (o) Pron, A.; Gawrys, P.; Zagorska, M.; Djurado, D.; Demadrille, R. *Chem. Soc. Rev.* **2010**, *39*, 2577–2632.

(16) Miyaura, N.; Suzuki, A. *Chem. Rev.* **1995**, *95*, 2457–2483.

(17) (a) Stille, J. K. *Angew. Chem., Int. Ed. Engl.* **1986**, *25*, 508–524.

(b) Kosugi, M.; Sasazawa, K.; Shimizu, Y.; Migita, T. *Chem. Lett.* **1977**, 301–302.

(18) (a) Hartwig, J. F. *Angew. Chem., Int. Ed.* **1998**, *37*, 2046–2067.

(b) Yang, B. H.; Buchwald, S. L. *J. Organomet. Chem.* **1999**, *576*, 125–146.

(19) Netherton, M. R.; Fu, G. C. *Org. Lett.* **2001**, *3*, 4295–4298.

(20) (a) Iwaoka, M.; Takemoto, S.; Okada, M.; Tomoda, S. *Bull. Chem. Soc. Jpn.* **2002**, *75*, 1611–1625. (b) Yasuda, T.; Sakai, Y.; Aramaki, S.; Yamamoto, T. *Chem. Mater.* **2005**, *17*, 6060–6068.

(21) Bondi, A. J. *Phys. Chem.* **1964**, *68*, 441–451.

(22) Fong, H. H.; So, S. K. *J. Appl. Phys.* **2005**, *98*, 023711–1–4.

(23) (a) Iino, H.; Takayashiki, Y.; Hanna, J.; Bushby, R. J.; Haarer, D.

*Appl. Phys. Lett.* **2005**, *87*, 192105–1–3. (b) Iino, H.; Hanna, J.; Haarer, D.

*Phys. Rev. B* **2005**, *72*, 193203–1–4. (c) Monobe, H.; Shimizu, Y.;

Okamoto, S.; Enomoto, H. *Mol. Cryst. Liq. Cryst.* **2007**, *476*, 31–41.

(d) Funahashi, M.; Hanna, J. *Appl. Phys. Lett.* **2000**, *76*, 2574–2576.

(e) van Breemen, A. J. J. M.; Herwig, P. T.; Chlon, C. H. T.; Sweelssen, J.;

Schoo, H. F. M.; Setayesh, S.; Hardeman, W. M.; Martin, C. A.;

de Leeuw, D. M.; Valetton, J. J. P.; Bastiaansen, C. W. M.; Broer, D. J.;

Popa-Merticaru, A. R.; Meskers, S. C. J. *J. Am. Chem. Soc.* **2006**,

*128*, 2336–2345. (f) Funahashi, M.; Zhang, F.; Tamaoki, N. *Adv. Mater.*

**2007**, *19*, 353–358. (g) Méry, S.; Haristoy, D.; Nicoud, J.-F.; Guillon, D.;

Diele, S.; Monobe, H.; Shimizu, Y. *J. Mater. Chem.* **2002**, *12*, 37–41.

(24) (a) Kulkarni, A. P.; Tonzola, C. J.; Babel, A.; Jenekhe, S. A. *Chem.*

*Mater.* **2004**, *16*, 4556–4573. (b) Hughes, G.; Bryce, M. R. *J. Mater. Chem.*

**2005**, *15*, 94–107.

(25) (a) Barth, S.; Müller, P.; Riel, H.; Seidler, P. F.; Rieß, W.;

Vestweber, H.; Bässler, H. *J. Appl. Phys.* **2001**, *89*, 3711–3719.

(b) Kepler, R. G.; Beeson, P. M.; Jacobs, S. J.; Anderson, R. A.; Sinclair,

M. B.; Valencia, V. S.; Cahill, P. A. *Appl. Phys. Lett.* **1995**, *66*, 3618–3620.

(c) Liao, S.-H.; Shiu, J.-R.; Liu, S.-W.; Yeh, S.-J.; Chen, Y.-H.; Chen,

C.-T.; Chow, T. J.; Wu, C.-I. *J. Am. Chem. Soc.* **2009**, *131*, 763–777.

(d) Yasuda, T.; Yamaguchi, Y.; Zou, D.-C.; Tsutsui, T. *Jpn. J. Appl. Phys.*

**2002**, *41*, S626–S629.

(26) (a) Ishi-i, T.; Yaguma, K.; Thiemann, T.; Yashima, M.; Ueno,

K.; Mataka, S. *Chem. Lett.* **2004**, *33*, 1244–1245. (b) Yamamoto, T.;

Watanabe, S.; Fukumoto, H.; Sato, M.; Tanaka, T. *Macromol. Rapid Commun.*

**2006**, *27*, 317–321. (c) Chen, H.-F.; Yang, S.-J.; Tsai, Z.-H.; Hung, W.-Y.;

Wang, T.-C.; Wong, K.-T. *J. Mater. Chem.* **2009**, *19*, 8112–8118.

(27) It has been suggested that in columnar phases, the rotational

motions of discotic molecules are much slower than is charge hopping

frequency between the stacked molecules: (a) Shen, X.; Dong, R. Y.;

Boden, N.; Bushby, R. J.; Martin, P. S.; Wood, A. *J. Chem. Phys.* **1998**,

*108*, 4324–4332. (b) Dong, R. Y.; Morcombe, C. R. *Liq. Cryst.* **2000**, *27*,

897–900.

(28) *N*-Thienylcarbazoles show the absorption maximum at 292 nm,

which is located at nearly the same point as the higher energy absorption

maximum of **2** ( $\lambda_{\text{abs}} = 299$  nm). See: Wu, I.-Y.; Lin, J. T.; Tao, Y.-T.;

Balasubramaniam, E. *Adv. Mater.* **2000**, *12*, 668–669.

(29) (a) Pommerehne, J.; Vestweber, H.; Guss, W.; Mahrt, R. F.;

Bässler, H.; Porsch, M.; Daub, J. *Adv. Mater.* **1995**, *7*, 551–554. (b) Yasuda,

T.; Imase, T.; Yamamoto, T. *Macromolecules* **2005**, *38*, 7378–7385.